Novel Lymphocyte-Independent Antitumor Activity by PD-1 Blocking Antibody against PD-1$^+$ Chemoresistant Lung Cancer Cells

Ramona Rotolo[1,2], Valeria Leuci[2], Chiara Donini[1,2], Federica Galvagno[1,2], Annamaria Massa[1,2], Maria Chiara De Santis[3], Serena Peirone[4,5], Giovanni Medico[1], Martina Sanlorenzo[6], Igor Vujic[7,8], Loretta Gammaitoni[2], Marco Basiricò[2], Luisella Righi[9], Chiara Riganti[1], Iris Chiara Salaroglio[1], Francesca Napoli[9], Fabrizio Tabbò[9], Annapaola Mariniello[9], Elisa Vigna[1,2], Chiara Modica[2,10], Lorenzo D'Ambrosio[9], Giovanni Grignani[2], Riccardo Taulli[1,11], Emilio Hirsch[3], Matteo Cereda[4,5], Massimo Aglietta[1,2], Giorgio Vittorio Scagliotti[9], Silvia Novello[9], Paolo Bironzo[9], and Dario Sangiolo[1,2]

ABSTRACT

Purpose: Antibodies against the lymphocyte PD-1 (aPD-1) receptor are cornerstone agents for advanced non–small cell lung cancer (NSCLC), based on their ability to restore the exhausted antitumor immune response. Our study reports a novel, lymphocyte-independent, therapeutic activity of aPD-1 against NSCLC, blocking the tumor-intrinsic PD-1 receptors on chemoresistant cells.

Experimental Design: PD-1 in NSCLC cells was explored *in vitro* at baseline, including stem-like pneumospheres, and following treatment with cisplatin both at transcriptional and protein levels. PD-1 signaling and RNA sequencing were assessed. The lymphocyte-independent antitumor activity of aPD-1 was explored *in vitro*, by PD-1 blockade and stimulation with soluble ligand (PD-L1s), and *in vivo* within NSCLC xenograft models.

Results: We showed the existence of PD-1$^+$ NSCLC cell subsets in cell lines and large *in silico* datasets (Cancer Cell Line Encyclopedia and The Cancer Genome Atlas). Cisplatin significantly increased PD-1 expression on chemo-surviving NSCLC cells (2.5-fold $P = 0.0014$), while the sequential treatment with anti–PD-1 Ab impaired their recovery after chemotherapy. PD-1 was found to be associated with tumor stemness features. PD-1 expression was enhanced in NSCLC stem-like pneumospheres ($P < 0.0001$), significantly promoted by stimulation with soluble PD-L1 ($+27\% \pm 4$, $P < 0.0001$) and inhibited by PD-1 blockade ($-30\% \pm 3$, $P < 0.0001$). The intravenous monotherapy with anti–PD-1 significantly inhibited tumor growth of NSCLC xenografts in immunodeficient mice, without the contribution of the immune system, and delayed the occurrence of chemoresistance when combined with cisplatin.

Conclusions: We report first evidence of a novel lymphocyte-independent activity of anti–PD-1 antibodies in NSCLC, capable of inhibiting chemo-surviving NSCLC cells and exploitable to contrast disease relapses following chemotherapy.

Introduction

In the last decade, the programmed cell death (PD-1) receptor emerged as a key immune regulator of T-cell response, becoming a target for cancer immunotherapy strategies with checkpoint inhibitors dramatically impacting on the treatment and outcome of patients with multiple types of solid tumors, including non–small cell lung cancer (NSCLC; ref. 1). The main underlying biological rationale implies that PD-1 is capable, upon binding its cognate ligands (PD-L1/2) on tumor cells and tumor microenvironment (TME), to directly inhibit T lymphocytes that may eventually be rescued into effective action by mAbs blocking the PD-1/PD-L1 axis (2–8). Besides this fundamental principle, it has been recently reported that PD-1 may also be expressed directly on the membrane of a subset of tumor cells with a supposed tumorigenic role and a consequent direct antitumor effect by PD-1 blockade (9). The first compelling evidence was generated in melanoma, where tumor-intrinsic PD-1 expression was found to be associated with stemness membrane markers and tumor-initiating features, promoted by PD-L1 binding and functionally inhibited by PD-1 blockade (10, 11). Mechanistically, PD-1 receptor pathways in tumor cells may promote the phosphorylation of ribosomal S6 protein and activate downstream mTOR signaling (10). PD-1 may be engaged by PD-L1 expressed on the surrounding tumor cells and TME elements, and/or on the same tumor cells establishing in cis binding (9, 12). Additional preclinical evidence supported the existence of such "ectopic" and protumorigenic PD-1 expression in pancreatic

[1]Department of Oncology, University of Turin, Torino, Italy. [2]Candiolo Cancer Institute FPO – IRCCS, Candiolo (Torino), Italy. [3]Department of Molecular Biotechnology and Health Sciences, Molecular Biotechnology Center, University of Torino, Torino, Italy. [4]Department of Biosciences, University of Milan, Milan, Italy. [5]Italian Institute for Genomic Medicine, c/o IRCCS, Candiolo (Torino), Italy. [6]Comprehensive Cancer Center, Institute of Cancer Research, Medical University of Vienna, Vienna, Austria. [7]The Rudolfstiftung Hospital, Vienna, Austria. [8]Faculty of Medicine and Dentistry, Danube Private University, Krems, Austria. [9]Department of Oncology, University of Turin, San Luigi Gonzaga Hospital, Orbassano (TO), Italy. [10]Department of Surgical, Oncological and Stomatological Sciences (DICHIRONS), University of Palermo, Palermo, Italy. [11]Center for Experimental Research and Medical Studies (CeRMS), City of Health and Science University Hospital di Torino, Torino, Italy.

R. Rotolo, V. Leuci, and C. Donini contributed as co-first authors and P. Bironzo and D. Sangiolo contributed as co-last authors of this article.

Corresponding Authors: Dario Sangiolo, University of Turin, Candiolo Cancer Institute FPO – IRCCS, Str. Provinciale 142 km 3.95, Candiolo 10060, Italy. Phone: 39 0119933521; Fax: 39 0119933522; E-mail: dario.sangiolo@ircc.it; and Chiara Donini, E-mail: chiara.donini@unito.it

Clin Cancer Res 2022;XX:XX–XX

doi: 10.1158/1078-0432.CCR-22-0761

Translational Relevance

We investigated and reported a novel lymphocyte-independent antitumor activity of anti–PD-1 antibodies (Ab) in non–small cell lung cancer (NSCLC) that is capable of inhibiting chemopersistent PD-1$^+$ NSCLC cells. The underlying rationale is the inhibition of the pro-tumorigenic PD-1 receptor directly expressed by a subset of NSCLC cells that are relatively chemoresistant to cisplatin and supposedly endowed with stemness features. In the clinical perspective, it would be conceivable to explore the activity of anti–PD-1 Abs to contrast the residual PD-1$^+$ NSCLC cells persistent after chemotherapy, with the intent of counteracting their promotion of disease relapse. Our findings support a new and clinically exploitable conception for the activity of PD-1 blocking Abs, not substitutive but integrative to the mainstream action based on the rescuing of exhausted T lymphocytes.

cancer, hepatocarcinoma, and bone and soft-tissue sarcomas (13–15). Initial evidence of PD-1$^+$ tumor cells has also been reported for lung cancer, but the prevalence of such cell subsets and the biological role are still unclear with even some contrasting findings (9, 12, 16, 17). The definition of tumor-intrinsic PD-1 in NSCLC could be of great clinical relevance, opening new perspectives and expanding the current therapeutic meaning of anti–PD-1 blocking antibodies. In advanced or metastatic NSCLC, anti–PD-1 treatment has significantly improved the outcome of patients and its role has been already acknowledged by therapeutic guidelines, either as monotherapy or in association with cytotoxic chemotherapy (18–24). However, disease relapse or refractoriness to immunotherapy still represents a relevant clinical challenge (20, 23). A deeper understanding of the intrinsic PD-1 role and the awareness of a novel direct effect of PD-1 blockade on tumor cells could fuel new rationale and possible schemas for designing effective therapeutic strategies.

We previously demonstrated that PD-1$^+$ melanoma cells are significantly enriched following treatment with BRAF/MEK inhibitors and that combination with anti–PD-1 antibody could prolong the antitumor response and delay disease relapse (25). Here we explore whether a similar principle may be applied to the field of NSCLC. We hypothesized that a tiny PD-1$^+$ tumor cell subset exists within NSCLC and, based on their relative chemoresistance, can be enriched to relevant rates following conventional treatments with potentially important implications in disease relapse. In line with this idea, we here define the extent of PD-1$^+$ NSCLC cells, their stemness and chemoresistance features and a novel, lymphocyte-independent, anti-NSCLC activity of anti–PD-1 blocking antibodies.

Materials and Methods

NSCLC cells and cultures

NSCLC cell lines were obtained from ATCC: six adenocarcinoma cell lines (H1975, H23, H820, HCC827, A549, H460) and three squamous cell carcinoma (EBC-1, H520, H596). Cell lines used were authenticated by genotype analysis with Cell_ID system (Promega) and comparing their profile with those published on the ATCC database and tested negative for *Mycoplasma* contamination by the Venor GeM Advance *Mycoplasma* Detection Kit (Minerva Biolabs) according to the manufacturer's instructions. Cell lines for experiments were obtained from the original cryopreserved golden stock and experiments performed immediately after or within the following month. All cell lines were cultured in RPMI (Sigma) supplemented with 10% FBS (EuroClone), 1% glutamine (Q; Gibco BRL), and 1% penicillin (100 U/mL) streptomycin (100 μg/mL; Sigma). Cells were maintained in a humidified 5% CO_2, incubator at 37°C.

Primary patient-derived NSCLC cell lines (SL-165, SL-166, LC-1) were generated from surgical tumor biopsies. Patients release informed consent approved by the internal review board ethics committee. Patient-derived cell lines tested negative for *Mycoplasma* contamination by the Venor GeM Advance *Mycoplasma* Detection Kit (Minerva Biolabs) according to the manufacturer's instructions. All the experiments were performed on patient-derived cell lines immediately after thawing or within the following month. Patient-derived NSCLC cell lines were maintained in F12 Nutri Mix HAM's (Gibco) supplemented with 10% di FBS (EuroClone), 1% di penicillin (100 U/mL) streptomycin (100 μg/mL; Sigma), and 5% di B-27 Supplement (GIBCO) in a humidified 5% CO_2, incubator at 37°C. Cells were harvested using Accutase solution (Gibco BRL).

Pneumospheres were generated seeding NSCLC cells in Ultra-Low Attachment flasks (Corning), in serum-free DMEM-F12 medium (Sigma) containing 20 ng/mL of FGF, 20 ng/mL epithelial growth factor, and 10% B-27 Supplement (GIBCO). Pneumospheres were disaggregated by vigorous pipetting with ethylenediaminetetraacetic acid 0.5 mmol/L.

PD-1 mRNA detection

Total RNA was extracted from all NSCLC cell lines cultured both in monolayer and in pneumospheres condition. RNA was extracted by Maxwell RSC Instrument (PR omega), according to Maxwell RSC RNA tissue Kit manufacturer instructions (PR omega). RNA was quantified by The Envoi DS-11 FX Series of Spectrophotometers/Fluorimeters. RNA retrotranscription was carried out by SuperScript II RT-PCR (Life Technologies, Inc.). PCR was performed with the specific primers 5′-ATGCATGGCTGGCTGCTCCT-3′ (forward) and 5′-TCAAAGAGGCCAAGAACAATGTC-3′ (reverse) for PDCD1 and HotStarTaq DNA Polymerase (QIAGEN). In selected cases, we sequenced amplified cDNA and confirmed the PD-1 identity of PCR product by Nucleotide Basic Local Alignment Search Tool (BLASTn) algorithm. Primers for detection of human PD-1 (*PDCD1*) by real-time qPCR were 5′-ATGCATGGCTGGCTGCTCCT-3′ (forward) and 5′-CCCTTAGCCAGTCTTCGATACAGC-3′ (reverse); primers for human OCT3/4 (*POU5F1*) were: 5′-ATGTGGGTCCGGCAGGT-3′ and 5′-TCAAAGAGGCCAAGAACAATGTC-3. Primers for detection of human PD-L1 (*CD274*) and human PD-L2 (*PDCD1LG2*) by real-time qPCR were, respectively, 5′-TGCCGACTACAAGCGAATTACTG-3′ (forward) and 5′-CTGCTTGTCCAGATGACTTCGG-3′ (reverse) and 5′-CTCGTTCCACATACCTCAAGTCC-3′ (forward) and 5′-CTGGAACCTTTAGGATGTGAGTG-3′ (reverse).

All samples were run in triplicate and assayed using the SYBR Green Master Mix (Applied Biosystems). The relative transcript levels were determined by 2^{-} $(-\Delta\Delta C_t)$ method.

Cancer Cell Line Encyclopedia

PD-1 RNA-sequencing (RNA-seq) expression data were selected and downloaded from Cancer Cell Line Encyclopedia (CCLE) dataset (http://www.broadinstitute.org/ccle, access June 2018). The dataset included 67 adenocarcinoma and 28 squamous cell carcinoma cell lines. The mRNA expression of TTF1 and cytokeratins (KRT5/6A)

were used as a positive expression control for lung adenocarcinoma and lung squamous cell carcinoma, respectively.

The Cancer Genome Atlas

We downloaded from The Cancer Genome Atlas (TCGA) portal the clinical data (clinical data, pathology report) and the mRNA sequencing data (gene) of the 585 lung adenocarcinoma and 504 lung squamous cell carcinoma samples included (https://portal.gdc.cancer.gov/, access June 2018). The mRNA sequencing data were available for 585 adenocarcinoma and 504 squamous cell carcinoma samples. Genes with fragments per kilobase of transcript per million fragments mapped (FPKM) values >0.1 were considered expressed. Among patient samples included in TCGA lung adenocarcinoma project (LUAD), we selected the 520 primary tumors and we linked each gene expression profile with the histologic report to exclude tumor samples with evidence of immune infiltration (data are available for 504 samples). Among the patient samples included in TCGA lung squamous cell carcinoma project (LUSC), we selected 506 primary tumors and we linked each gene expression profile with the histologic report to exclude the samples with evidence of immune infiltration (data available for 501 samples).

Flow cytometry

Flow-cytometry acquisitions were performed using a CyanADP cytometer (Beckman Coulter s.r.l.). NSCLC cells were stained with APC fluorochrome-conjugated anti–PD-1 mAb (clone MIH4, BD Biosciences). An isotype control IgG1 was suitable as a negative control to set gate of positive staining. Analyses were performed using Summit Software.

Immunofluorescence staining

Immunofluorescence staining was performed on pneumospheres fixed in 4% paraformaldehyde for 1 hour and applied on polylisynate glass slides. Fixed pneumospheres were permeabilized with 0.2% PBS-Triton. Pneumospheres were stained with primary antibodies specific for PD-1, PD-L1, and PD-L2 (D4W2J XP PD-1 Rabbit mAb, E1L3N XP PD-L1 Rabbit mAb, and D7U8C XP PD-L2 Rabbit mAb, Cell Signaling Technology) overnight and subsequently incubated 1 hour with anti-Rabbit secondary antibody conjugated with AF555 fluorocrome. Nuclei were stained with DAPI. Pneumospheres were observed using confocal laser-scanning microscope (Leica SPIIE, Leica Microsystems). Image acquisition of pneumospheres was performed maintaining the same laser power, gain, offset, and magnification (20×) setting. Images were analyzed using ImageJ software.

Western blot analysis

Protein samples were resuspended in Laemmli buffer, boiled 15 minutes at 95°C and resolved by SDS-PAGE. Membranes probed with the indicated antibodies were then incubated with horseradish peroxidase (HRP)-conjugated secondary antibodies (anti-mouse used 1:10,000, anti-rabbit 1:5,000, Sigma) and developed with enhanced chemiluminescence (Clarity Max Western ECL Substrate, 1705062, Bio-Rad). The following primary antibodies were used: Phospho-p70 S6 Kinase (Thr389) 15 (Rabbit, #9234, Cell Signaling Technology), p70 S6 Kinase (Rabbit, #9202, Cell Signaling Technology), Phospho-S6 Ribosomal Protein (Ser235/236; 91B2; Rabbit, #4857, Cell Signaling Technology), S6 Ribosomal Protein (5G10; Rabbit, #2217, Cell Signaling Technology), Phospho-Akt (Ser473; Rabbit, 19 #9271, Cell Signaling Technology), Akt (pan; 40D4; Mouse, #2920, Cell Signaling Technology), Vinculin (Mouse, sc-25336), Phospho-p44/42 MAPK (Erk1/2; Thr202/Tyr204; 20G11; Rabbit, #4376, Cell Signaling Technology), p44/42 MAPK (Erk1/2; Rabbit, 25 #9102, Cell Signaling Technology). Expression levels of phosphorylated versus total ERK1/2, AKT, S6K, and S6 ribosomal protein were determined in sorted H1975 PD-1^+ or PD-1^- cells in presence or absence of anti–PD-1 mAb (100 μg/mL) following subsequent incubation with or without recombinant PD-L1 Ig (25 μg/mL, 0% FBS for 15 minutes).

For phosho-p38 MAPK evaluation, total protein extracts were obtained by lysing cells using RIPA Buffer (Sigma-Aldrich). Western blotting was performed separating 30 μg of proteins by SDS-PAGE and electroblotting onto nitrocellulose membranes (Bio-Rad). Luminescence was revealed with a chemiluminescence reagent (Euroclone). Anti-rabbit antibodies linked with HRPs p38-p-MAPK (Tyr 202–204), p38-MAPK, and Vinculin were from Cell Signaling Technology.

Pneumosphere-forming capability assays

NSCLC pneumosphere cultures were established as described above. Cells were plated in the presence of anti-human PD-1 mAb [100 μg/mL, inVivoMAb anti-human PD-1 (CD279, Clone: J110, Bio X Cell) or isotype control mAb (100 μg/mL, inVivoMAb mouse IgG1 isotype control, Clone: MOPC-21, Bio X Cell) or synthetic PD-L1 soluble form (PD-L1s) (25 μg/mL, R&D Systems] in ultra-low attachment plates (Corning) at a density of 1,000 viable cells per well and cultured for 10 days at 37°C, 5% CO_2. Anti–PD-1 and isotype control mAbs or recombinant PD-L1s were restored every 3 days.

Pneumosphere-forming capability was determined by counting the number of pneumospheres originated from the specific number of plated cells using a light microscope (Leika) 10 days after seeding (images taken at 40× magnification). In selected experiments, we used an automated live-cell imaging system (Nikon's LIPSI). To efficiently and rapidly detect pneumospheres, we set up a simple imaging pipeline: cells were labeled with NucBlue (NucBlue Live Ready Probes Reagent) directly in the culture well plates and then put under a widefield microscope and illuminated with proper wavelengths and optical filters with a 4X objective and a motorized stage to cover the entire well. Digital images were then processed according to a custom-made simple image analysis algorithm written for Fiji (ImageJ 2.0.0-rc-69/1.52p; Java1.8.0_172). Briefly, images were binarized using Otsu method, objects touching the borders of the image were automatically removed and the binary components were filtered to exclude objects larger than 36 or smaller than 65 μm^2. The remaining objects were automatically counted and the average size was computed.

Library preparation, sequencing, and data analysis

NSCLC pneumosphere cultures were established, as described above. NSCLC pneumospheres were stimulated by synthetic PD-L1s (25 μg/mL, R&D Systems) in 0% FBS culture medium for 15 minutes.

RNA was extracted from NSCLC pneumospheres by Maxwell RSC Instrument, according to Maxwell RSC RNA tissue Kit manufacturer instructions.

RNA-seq library was generated from 0.1 μg of RNA using Illumina Total RNA Prep Stranded Ligation with Ribo-Zero according to manufacturer's recommendations. Libraries were sequenced on Illumina NovaSeq6000 in 100-nt-long paired-end read modality.

Raw sequencing reads were aligned to the human genome reference GENCODE GRCh37 version 28 (26) using STAR v.2.7.3a (27) in basic two-pass mode using the following parameters: –alignInsertionFlush Right –outSAMstrandField intronMotif –outSAMattributes NH HI NM MD AS XS –peOverlapNbasesMin

20 –peOverlapMMp 0.25 –chimSegmentMin 12 –chimJunctionOverhangMin 8 –chimOutJunctionFormat 1 –chimMultimapScoreRange 3 –chimScoreJunctionNonGTAG -4 –chimMultimapNmax 20 –chimNonchimScoreDropMin 10 –outFilterIntronStrands RemoveInconsistentStrands –outFilterMultimapNmax 1 –bamRemoveDuplicatesType UniqueIdentical. Raw read counts were estimated using featureCounts from Subread v. 2.0.0 (28) with parameters -O –primary -Q 1 -J -s 2 -p -B. Protein coding genes were selected ($N = 20{,}298$). A batch correction to account for genetic heterogeneity of cell lines from distinct patient was applied using CombatSeq function from R package "sva" (29). Differential expression analysis was performed using the "DESeq2" R package (30) comparing the PD-L1s treated versus untreated NSCLC pneumospheres. Genes that presented an absolute $\log_2$(fold change)>1 and an adjusted P value ≤0.05 were considered as differentially expressed.

PD-1 mRNA downregulation by RNAi

PD-1 downregulation was established using RNAi system. H1975 cells were transduced with three different bicistronic lentiviral vectors LV-pGFP-C-shRNA (OriGene), encoding for different shRNA-PD-1 cassettes and for eGFP protein. H1975 cells were infected adding virus-conditioned medium where each lentivirus preparation was used at the dose of 2 multiplicity of infection. NSCLC cell lines transduced with lentivirus LV-pGFP-C-MOCK (OriGene) were used as control. After 16 hours, cells were washed twice and grown for 7 days. Transduction efficiency was assessed on the basis of GFP expression by CyanADP cytometer (Dako). PD-1 mRNA downregulation was explored by qRT-PCR as described above.

NSCLC cell proliferation rate after treatment with cisplatin

NSCLC cells were plated in standard culture condition at a density of 1×10^5 viable cells per well. After 24 hours, cells were treated with cisplatin (CDDP) at estimated IC_{50} and cultured at 37°C, 5% CO_2 for 72 hours. After CDDP treatment, surviving cells were stained with APC fluorochrome-conjugated anti–PD-1 mAb (clone MIH4, BD Biosciences) and the percentage of PD-1^+ cells was assessed by CyanADP cytometer (Beckman Coulter s.r.l.). In parallel, NSCLC cells surviving to CDDP treatment were seeded both in pneumosphere-promoting conditions and in standard culture condition in the presence of blocking PD-1 mAb [100 μg/mL, inVivoMAb anti-human PD-1(CD279), Clone: J110, Bio X Cell] or isotype control mAb (100 μg/mL, inVivoMAb mouse IgG1 isotype control, Clone: MOPC-21, Bio X Cell). Anti–PD-1 or isotype control mAbs were restored every 3 days. Monolayer tumor cell growth and number of pneumospheres were determined by direct count with a light microscope (Leika) at 10 days after treatment with anti–PD-1 antibody.

To perform colony-forming unit assay, NSCLC cells surviving to CDDP treatment were treated by PD-1 mAb [100 μg/mL, inVivoMAb anti-human PD-1(CD279), Clone: J110, Bio X Cell] or isotype control mAb (100 μg/mL, inVivoMAb mouse IgG1 isotype control, Clone: MOPC-21, Bio X Cell). Colonies derived from a single cell [colony-forming unit (CFU)] were obtained by plating 500 cells per well in 24-well plates in appropriate culture medium. After 10 days, the culture medium was removed and a PBS wash was performed. Cells were fixed with 2.5% glutaraldehyde and incubated for 20 minutes. The colonies were then stained with 0.1% crystal violet. The image of the entire plate was acquired through Chemidoc (Bio-Rad); furthermore, CFUs into wells were counted with the optical microscope.

In vivo anti–PD-1 antitumor effect

The antitumor activity of anti–PD-1 blocking Ab was explored within two NSCLC xenograft models in immunodeficient mice [NOD.Cg-Prkdcscid Il2rgtm1Wjl/SzJ (NSG)] purchased from Charles River Laboratories Italia s.r.l. (Calco - Lecco, Italy). Mice were injected subcutaneously with 1×10^6 H1975 or EBC-1 NSCLC cells and assigned to treatment groups. Treatments started either 2 days after tumor cell implantation (model 1, EBC-1) or when palpable tumor masses became evident (model 2, H1975).

CDDP was administered by tail vein injection once a week at a dose of 5 mg/Kg. Anti–PD-1 Ab and the respective isotype control were injected intraperitoneally (200 μg per injection) three times a week. Mice were sacrificed when the main tumor diameter reached 2 cm or ulceration occurred. All procedures were performed according to the Institutional Review Board–approved protocols.

Statistical analysis

Data were analyzed using GraphPad Prism Version 8 (GraphPad Software). Descriptive data are presented as mean or median values ± SEs. In the comparison of two groups, statistical significance was evaluated by nonparametric t test (Mann–Whitney test). $P < 0.05$ was considered significant. For comparison of three or more groups, the data were analyzed by two-way ANOVA with Bonferroni multiple comparison posttests. A P value < 0.05 was considered significant. Significance is represented on graphs as *, $P \le 0.05$; **, $P \le 0.01$; ***, $P \le 0.001$; and ****, $P \le 0.0001$.

Data availability

The RNA-seq data generated in this study are publicly available in Gene Expression Omnibus at GSE210516 and in Code Ocean at https://codeocean.com/capsule/0588225/tree/v1.

Results

PD-1 receptor is intrinsically expressed by a subset of chemoresistant NSCLC cells enriched after CDDP

The intrinsic expression of PD-1 receptor by a subset of NSCLC cells was first detected by flow cytometry in 12 human NSCLC cell lines: nine adenocarcinomas including three primary patient-derived cell lines (H1975, H23, H820, HCC827, A549, H460, SL165, SL166, LC-1), and three squamous cell carcinoma cell lines (EBC-1, H520, H596). We found the presence of a small PD-1^+ subset in all 12 NSCLC cell lines (mean 4% ± 0.3, $n = 12$; **Fig. 1A** and **B**). Tumor PD-1 expression was confirmed, at molecular level, by RT-PCR (**Fig. 1C**) and its identity confirmed by sequencing the PCR product. To validate our results, we explored the intrinsic NSCLC expression of PD-1 mRNA by *in silico* analysis of data extracted from CCLE and TCGA. In CCLE are included 136 NSCLC cell lines. Of those PD-1 was expressed in all 67 adenocarcinomas analyzed [Affimetryx RNA value 4,348 (3,882–6,361)] and 28 squamous cell carcinomas [Affimetryx RNA value 4,338 (3,995–5,178)]. In most of the NSCLC cell lines, the levels of PD-1 RNA were comparable with those found for the PD-1 ligands (PD-L1, PD-L2; **Fig. 1D**). In TCGA dataset are included 585 lung adenocarcinoma and 504 lung squamous cell carcinoma samples, we linked each gene expression profile with the histologic report to exclude the samples with evidence of immune infiltration. PD-1 was expressed in 278 lung adenocarcinoma [median FPKM values 5.8 (1.0–8.7)] and in 401 lung squamous cell carcinoma [median FPKM values 5.4 (0–10.0)]. In all the selected samples, we also determined the expression of PDL-1 and PDL-2 in both adenocarcinoma

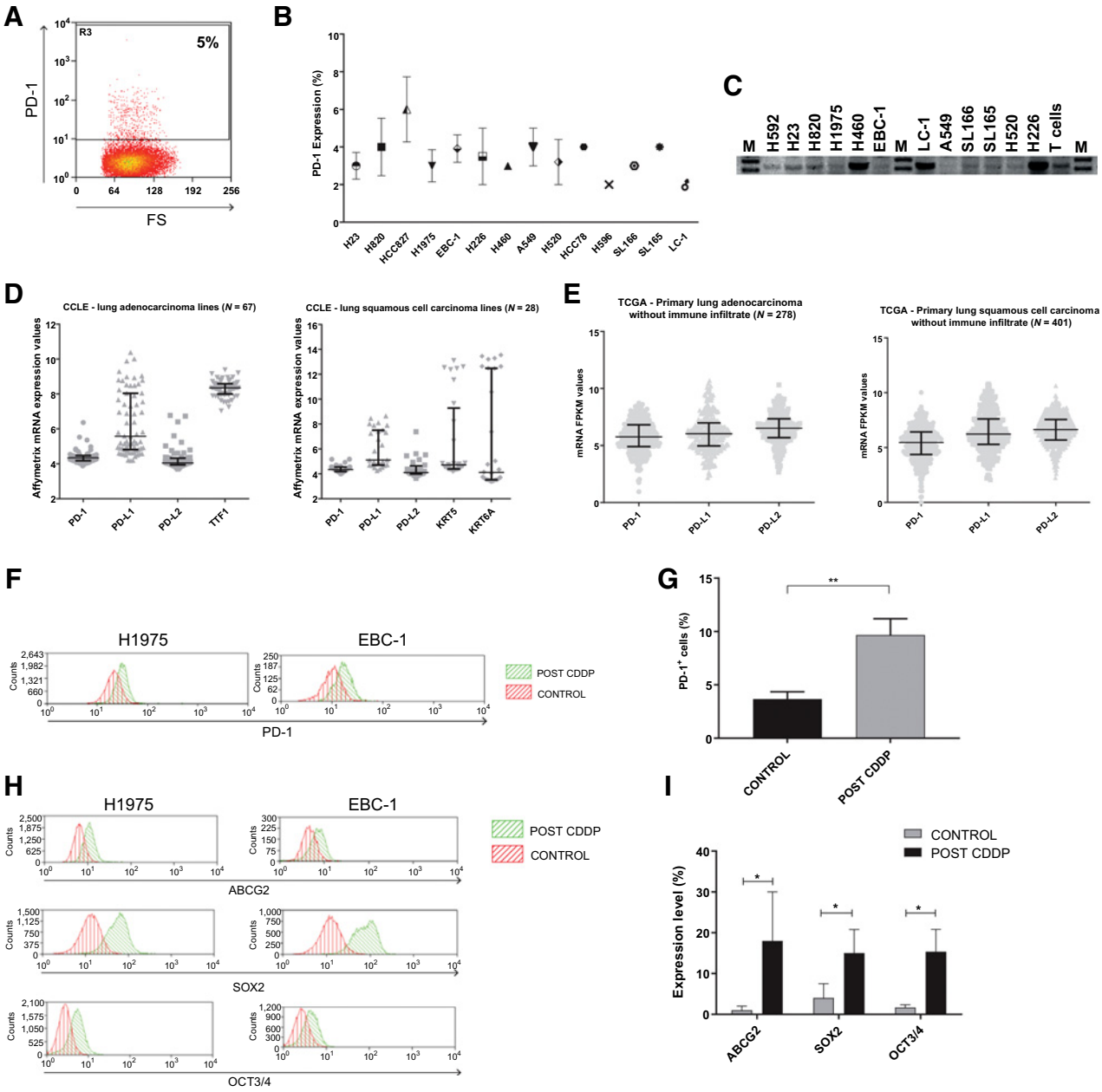

Figure 1.

Baseline subsets of PD-1$^+$ NSCLC cells and their enrichment after CDDP. We reported the existence of a PD-1$^+$ tumor cell subset in 12 different NSCLC cell lines. A representative flow cytometry plot (**A**) and mean (±SEM) values of membrane PD-1 expression (**B**) are reported. The finding was confirmed at the transcriptional level; expression of PD-1 mRNA in the same NSCLC cell lines (**C**) is reported, with T lymphocytes used as positive control. The presence of tumor cell intrinsic PD-1 was confirmed on large *in silico* datasets. Affymetrix mRNA expression values of PD-1, PD-L1, and PD-L2 in lung adenocarcinoma ($n = 67$) and squamous cell carcinoma ($n = 28$) cell lines included in CCLE are reported (**D**); TTF1 and KRT5/5A were used as referral control. Similarly, mRNA expression values of PD-1, PD-L1, and PD-L2 of lung adenocarcinoma ($n = 278$) and squamous carcinoma ($n = 401$) patient samples extracted from TCGA, excluding those with histologic evidence of immune infiltrates, were analyzed and reported (**E**). The subset of PD-1$^+$ NSCLC cells significantly increased after treatment *in vitro* with CDDP ($P = 0.0014$); representative flow cytometry histograms (**F**) and cumulative data (**G**) are reported. A parallel increase in the expression of three main stem-related genes (ABCG2, SOX2, OCT3/4) was reported after treatment with CDDP *in vitro*; representative flow cytometry histograms (**H**) and cumulative data (**I**) are reported. Results were analyzed by *t* test. A *P* value ≤ 0.05 was considered significant; statistical significance is reported as *, $P \leq 0.05$; **, $P \leq 0.01$; ***, $P \leq 0.001$; and ****, $P \leq 0.0001$.

[median FPKM values 6.0 (2.2–10.7) and 6.5 (2.7–10.3)] and squamous cell carcinomas [median FPKM values 6.2 (2.1–10.8) and 6.6 (2.3–10.6)] (**Fig. 1E**).

From a functional perspective we hypothesized that, similarly to what recently reported for melanoma, the tumor expression of PD-1 might characterize a subset of NSCLC cells with reduced sensitivity to conventional treatments. We treated NSCLC cells with CDDP for 72 hours at the IC_{50} dose. At the end of treatment, in all of the NSCLC cell lines tested the rate of PD-1$^+$ cells significantly increased among chemo-surviving NSCLC cells as compared with untreated control (2.5 ± 0.3 fold, $n = 4$, $P = 0{,}0014$; **Fig. 1F** and **G**). In the same experiments, along with the enrichment of PD-1$^+$ NSCLC cells, we demonstrated the contextual enhanced expression of three main stem-related genes (ABCG2, SOX2, OCT3/4; **Fig. 1H** and **I**), where ABCG2 is also associated with multidrug resistance features. In a selected assay, we observed by flow cytometry that OCT3/4 expression, as expected present at very low rates in the bulk cell population (0.5%–1% of the total cells), preferentially colocalized on PD-1$^+$ NSCLC cells as compared with the PD-1$^-$ counterpart (14% vs. 0.1%; Supplementary Fig. S1A).

PD-1 expression is enhanced in NSCLC stem-like cells

In melanoma, PD-1 has been reported to be preferentially expressed by a small fraction of tumor cells, with stem-like features endowed with a higher tumorigeneicity (10). To investigate whether PD-1 may have a similar expression pattern in NSCLC, we explored the intrinsic tumor expression of PD-1 on NSCLC cultured in stem-like pneumosphere-promoting conditions (31, 32). We found a significant increase of PD-1 expression on stem-like pneumospheres compared with paired monolayer controls cultured in standard conditions [median value 12% (4–36) vs. 2% (1–5), $P < 0{,}0001$, $n = 6$] (**Fig. 2A** and **B**). Higher expressions of PD-1 on stem-like pneumospheres were paralleled by the relative mRNA enrichment of the stem gene OCT4 (**Fig. 2C**) as compared with paired monolayer controls. PD-1 expression on pneumospheres was also confirmed and visualized by immunofluorescence (**Fig. 2D**).

Considering the potential activation of an intratumoral PD-1/PD-1 ligands (PD-L1/L2) axis in stem-like NSCLC cells, we confirmed the expression of PD-L1/L2 on NSCLC pneumospheres by real-time PCR. PD-L1/L2 levels resulted comparable with PD-1 expression on NSCLC pneumospheres (**Fig. 2E**). PD-L1/L2 expression on NSCLC

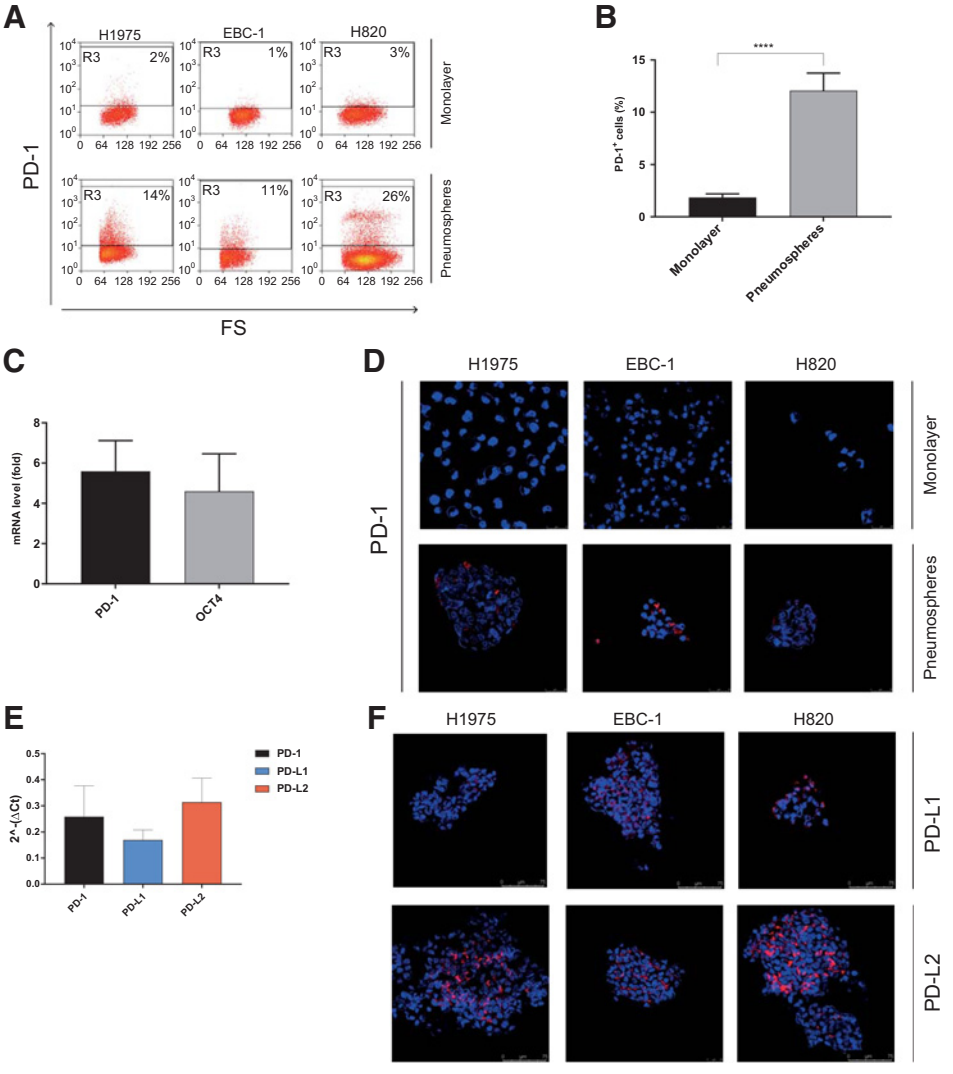

Figure 2.

Tumor PD-1 expression is enhanced in stem-like NSCLC pneumospheres. Tumor cell–intrinsic PD-1 expression *in vitro* resulted in enhanced stemness conditions. Representative flow cytometry plots with the basal rate of PD-1 expression in three NSCLC cell lines (top) and their enrichment in paired stem-like pneumospheres (bottom; **A**), as well as cumulative data ($P < 0.0001$, $n = 6$; **B**), are reported. The increase of PD-1 in NSCLC stem-like pneumospheres was confirmed at the transcriptional level, and it was paralleled by a comparable enhancement of the stem-gene Oct4 mRNA (**C**). The spatial distribution of PD-1 in NSCLC cells and their corresponding stem-like pneumospheres were visualized by immunofluorescence (AF 555, red). Nuclei are visualized by staining with 4′,6-diamidino-2-phenylindole (blue; **D**). Real-time PCR of expression levels of PD-1 and its main ligands, PD-L1/L2, on NSCLC pneumospheres (**E**). The spatial distribution of PD-L1 and PD-L2 in NSCLC stem-like pnemospheres was visualized by immunofluorescence (AF 555, red). Nuclei are visualized by staining with 4′,6-diamidino-2-phenylindole (blue; **F**). Results were analyzed by *t* test. A *P* value ≤ 0.05 was considered significant; statistical significance is reported as *, $P \le 0.05$; **, $P \le 0.01$; ***, $P \le 0.001$; and ****, $P \le 0.0001$.

pneumospheres was also confirmed and visualized by immunofluorescence (**Fig. 2F**).

PD-1$^+$ NSCLC stem-like pneumospheres are enhanced by PD-L1 stimulation and impaired by PD-1 blockade

To demonstrate a functional role of tumor PD-1 on stem-like NSCLC cells, we explored *in vitro* the effect of either PD-L1 binding or PD-1 blockade on NSCLC pneumospheres (**Fig. 3A**). The experimental treatment with a synthetic PD-L1s significantly promoted the stem-like pneumosphere-forming capability compared with paired unstimulated controls (27% ± 4, $n = 4$, $P < 0.0001$; **Fig. 3B**). Consistently, we found that PD-1 blockade, by anti–PD-1 antibody, significantly inhibited the generation of stem-like pneumospheres compared with paired controls (−30% ± 3, $n = 6$, $P < 0.0001$; **Fig. 3B**). In selected experiments, results were confirmed and visualized by automated live-cell imaging system (Nikon LIPSI). The number of NSCLC stem-like pneumospheres was significantly reduced by anti–PD-1 blocking antibody as compared with paired controls (−58%, $P = 0.02$, $n = 4$; **Fig. 3C** and **D**). In addition, we observed that PD-1 blockade also significantly impaired the size of pneumospheres compared with paired controls (54% ± 8.6 size reduction, $n = 3$, $P = 0.01$; **Fig. 3E**).

To downregulate PD-1 expression in NSCLC cells, we transduced the H1975 cell line with a lentiviral vector encoding for short hairpin RNAs (shRNA) targeting PD-1 (PD-1 shRNA H1975). We obtained a significant reduction of the PD-1 mRNA expression (−70%) and PD-1 protein (−66%) compared with control (wild type H1975; **Fig. 3F**). PD-1 shRNA H1975 cells showed a spontaneous reduction in the generation of stem-like pneumospheres, comparable with what observed with their parental counterpart when treated with anti–PD-1 antibody ($n = 3$; $P = 0.05$; **Fig. 3G**). Consistently, the stimulation with PD-L1s failed to enhance the number of stem-like pneumospheres from PD-1 shRNA H1975 (**Fig. 3H**).

Furthermore, we found by RNA-seq that treatment of pneumospheres ($n = 4$, H23, EBC-1, H820, H1975) *in vitro* with PD-L1s was associated with the significant upregulation of expression of 14 key protein coding genes, of which 11 have been reported to be involved in processes of tumorigenesis, epithelial–mesenchymal transition (EMT), tumor aggressiveness, and chemoresistance in various tumor settings (*RRM2, DUSP1, EGR1, HIST1H2AH, FOS, CTGF, DHRS2, UNC5A, DUSP2, FOSB, NPTX1*; refs. 33–48; Supplementary Fig. S2A and B).

Treatment with anti–PD-1 blocking antibody has lymphocyte-independent activity against NSCLC *in vitro* and *in vivo*

We hypothesized and explored the therapeutic antitumor activity of anti–PD-1 blocking antibody in absence of any contribution provided by the immune system. As a first step, we set an experiment where NSCLC cells were first treated *in vitro* with CDDP (IC_{50} dose), sequentially followed by anti–PD-1 Ab (100 μg/mL), with the intent of exploiting the observed enrichment of PD-1$^+$ NSCLC cells after chemotherapy. The sequential treatment with anti–PD-1 antibody significantly inhibited the proliferative regrowth of NSCLC cells surviving to CDDP ($n = 4$ H1975, EBC-1, H23, H820, $P = 0{,}005$) and at the same time impaired their capability to generate stem-like pneumospheres (240 vs. 368, $n = 4$ H1975, EBC-1, H23, H820, $P = 0.005$; **Fig. 4A** and **B**).

The sequential treatment with anti–PD-1 antibody inhibited also the clonogenic CFUs capability *in vitro* of NSCLC cells ($n = 2$; H1975 $P = 0.003$; EBC-1 $P = 0.03$; **Fig. 4C** and **D**).

In selected experiments ($n = 2$), the reduced sensitivity to CDDP was confirmed on sorted PD-1+ NSCLC cells as compared with the PD-1$^-$ counterpart ($n = 2$, $P = 0.001$; **Fig. 4E**).

We investigated changes of phosphor(p)-ERK1/2, p-AKT, and p-S6 ribosomal protein levels in NSCLC cells (H1975) in presence or absence of anti–PD-1 and PD-L1s, after sorting the PD-1$^+$ and PD-1$^-$subsets.

We observed the reduction of phosphor(p) p-S6 ribosomal protein levels following treatment with Ab anti–PD-1 in sorted PD-1$^+$ NSCLC cells as compared with the PD-1$^-$ counterpart, not rescued by the treatment with PD-L1s (**Fig. 4F**). We could not detect any significant variation for pAKT or pERK, with only a modest increasing trend for pAKT following treatment with Ab anti–PD-1.

Next, we explored *in vivo* the lymphocyte-independent antitumor activity of anti–PD-1 blocking Ab within two different models of NSCLC xenografts (EBC-1; H1975). The choice of complete immunodeficient [IL2r]γnull (NSG) mice was functional to ensure that the observed activity of PD-1 blockade could not be mediated by the well-known effect on antitumor T lymphocytes, but instead exerted directly on PD-1$^+$ NSCLC cells. In the first model, we observed that the intraperitoneal infusion of anti–PD-1 Ab as monotherapy (200 μg per injection), started at the same time of tumor xenograft implantation (EBC-1), significantly delayed tumor growth as compared with untreated controls ($n = 4$; $P = 0.0006$; **Fig. 5A** and **B**).

In a second experiment, the anti-NSCLC activity of Ab anti–PD-1 resulted comparable with that observed with monotherapy CDDP ($n = 4$, $P = 0.2$; **Fig. 5C–E**). The combination of Ab anti–PD-1 with CDDP showed a trend toward enhanced antitumor activity and delayed onset of chemoresistance, even if statistical significance was not reached ($n = 4$. 37 vs. 102 mm^3, $P = 0.5$; **Fig. 5C–E**).

In a second model, we confirmed the lymphocyte-independent activity of anti–PD-1 Ab even when infused to treat established and palpable NSCLC xenografts (H1975; $n = 6$, $P = 0.003$) as compared with untreated controls (**Fig. 6 A** and **B**). We confirm that the anti-NSCLC activity of Ab anti–PD-1 was comparable with that observed with monotherapy CDDP ($n = 6$, $P = 0.9$; **Fig. 6A** and **B**) also for established and palpable NSCLC xenografts. A trend toward enhanced antitumor activity and delayed onset of chemoresistance was observed with the combination of Ab anti–PD-1 with CDDP (550 vs. 729 mm^3, $P = 0.9$; **Fig. 6C**), even if statistical significance was not reached. In the same experiment, to support our hypothesis, in selected animals ($n = 2$) we could confirm the enrichment of PD-1$^+$ NSCLC following the treatment *in vivo* with CDDP monotherapy ($P = 0.03$; **Fig. 6D**).

Discussion

In this study, we investigated and described a novel, lymphocyte-independent, antitumor activity of anti–PD-1 antibody in NSCLC. It leverages on the inhibition of the PD-1 receptor directly expressed by a subset of NSCLC cells, relatively chemoresistant to CDDP and supposedly endowed with stemness features. Our findings support a new way of conceiving the activity of PD-1 checkpoint inhibitors, obviously not substitutive but integrative to the mainstream action based on the rescuing of exhausted T lymphocytes.

The PD-1 receptor, besides the well-known expression by T lymphocytes, is in fact apparently expressed by a small but constantly present subset of NSCLC cells.

The first point emerging from our study is indeed the demonstration of the existence of PD-1$^+$ NSCLC cell subsets, confirmed at both

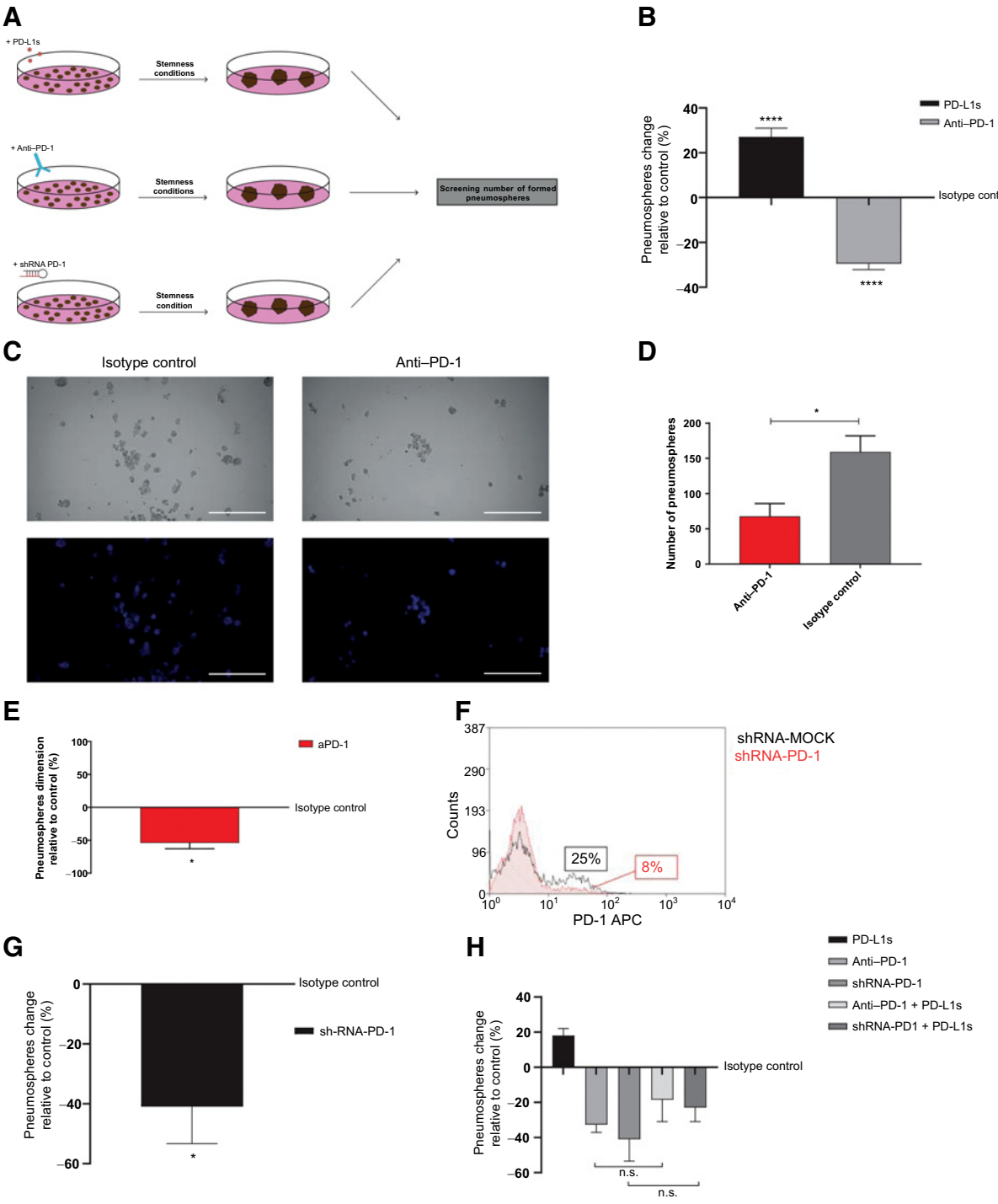

Figure 3.

NSCLC stem-like pneumospheres are promoted by PD-L1s and inhibited by PD-1 blockade. A schematic representation of the main experimental design to functionally investigate the effect of PD-1 stimulation or inhibition on NSCLC stem-like pneumospheres is reported (**A**). The capability of NSCLC cells to generate stem-like pneumospheres was significantly promoted ($P < 0.0001$) upon their stimulation with PD-L1s; consistently it was instead impaired ($P < 0.0001$) by PD-1 blockage (**B**). The reduced capability by NSCLC cells to generate pneumospheres by PD-1 blockage was confirmed and visualized by automated live-cell imaging system (Nikon's LIPSI). Representative images (**C**) and cumulative data (**D**) are reported ($n = 3$; $P = 0.02$; magnification 10×; scale bar: 500 μm). Treatment with anti–PD-1 blocking antibody also significantly impaired the size of newly generated pneumospheres ($n = 3$; $P = 0.01$; **E**). The genetic downregulation of PD-1, by PD-1 shRNA (**F**), consistently affected the generation of NSCLC stem-like pneumospheres ($n = 3$; $P = 0.05$; **G**). The functional effects by stimulation with PD-L1s or inhibition with anti–PD-1 blocking antibody on the ability to generate stem-like pneumospheres by (PD-1 shRNA) H1975 cell line is reported (**H**). Results were analyzed by *t* test. A *P* value ≤ 0.05 was considered significant; statistical significance is reported as *, $P \leq 0.05$; **, $P \leq 0.01$; ***, $P \leq 0.001$; and ****, $P \leq 0.0001$.

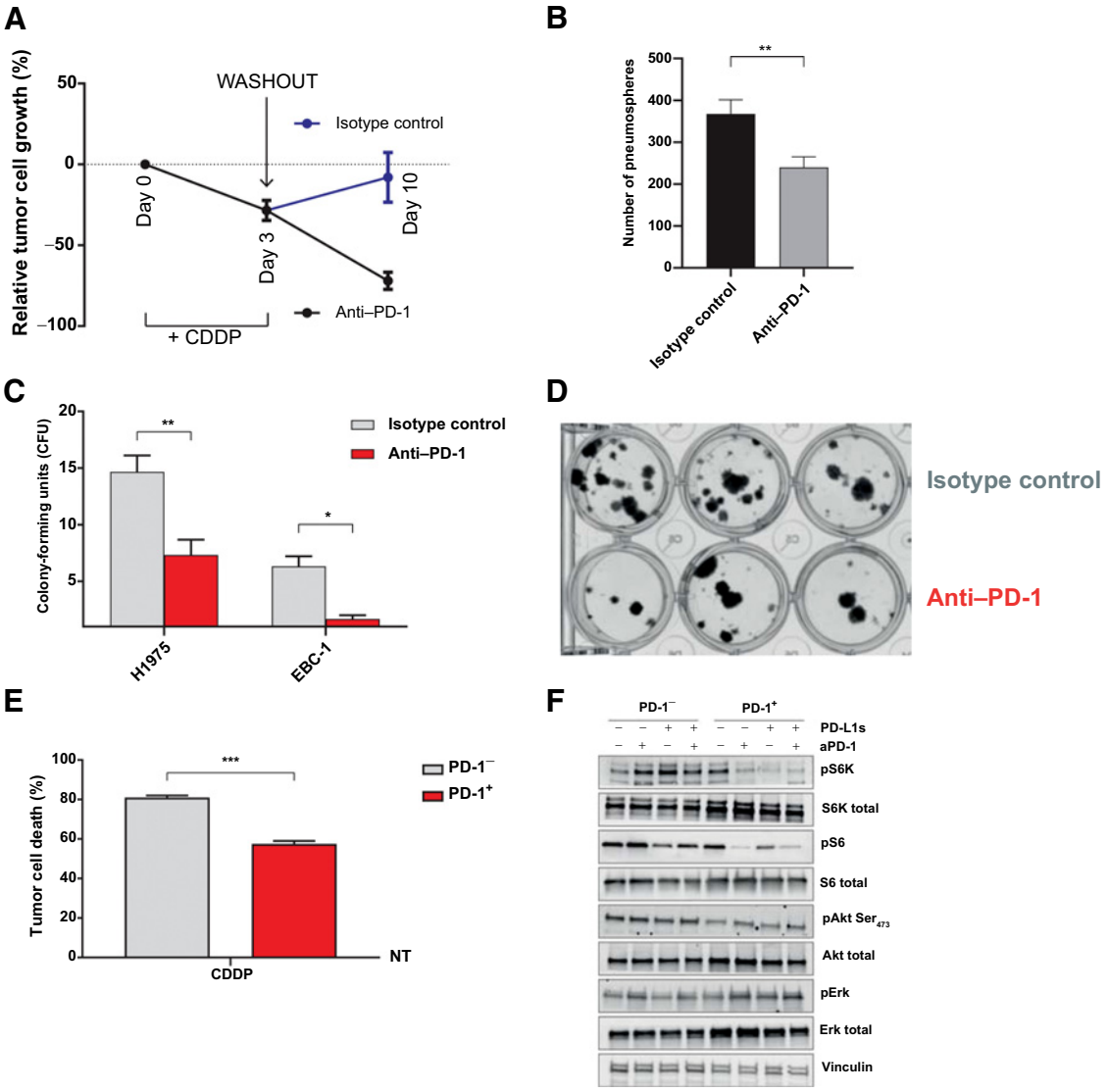

Figure 4.

Anti–PD-1 antibody impairs the recovery of PD-1$^+$ NSCLC cells resistant to CDDP. Treatment in vitro with anti–PD-1 antibody of chemo-surviving NSCLC cells significantly reduced both their proliferation ($n = 4$ H1975, EBC-1, H23, H820; $P = 0.005$; **A**) and capability to generate stem-like pneumospheres ($n = 4$ H1975, EBC-1, H23, H820; $P = 0.005$) after 10 days. **B,** Quantification of number of CFUs of NSCLC cells treated by anti–PD-1 antibody compared with isotype control ($n = 2$; H1975 $P = 0.003$; EBC-1; $P = 0.03$) after 10 days (**C**). Representative image of CFU assay on H1975 cells (**D**). Viability of PD-1$^+$ and PD-1$^-$ NSCLC cells after CDDP treatment ($n = 2$, $P = 0.001$; **E**). Immunoblot analysis of phosphorylated (p) and total S6K, S6, AKT, and ERK in sorted PD-1$^+$ and PD-1$^-$ NSCLC cells (H1975) with or without treatment by anti–PD-1 and/or PD-L1s ($n = 2$ independent experiments; **F**). Results were analyzed by *t* test. A *P* value ≤ 0.05 was considered significant; statistical significance is reported as *, $P \le 0.05$; **, $P \le 0.01$; ***, $P \le 0.001$; and ****, $P \le 0.0001$.

transcriptional and protein level. The low rate of the PD-1$^+$ tumor cells likely explain why they went so far almost unnoticed or considered negligible.

The underlying hypothesis is that this PD-1$^+$ tumor cell subset, supposedly associated with stemness features, is represented only by a small number of cells in tumor steady conditions but it may increase in specific situations becoming relevant for tumor homeostasis and chemotherapy resistance. This is in line with what was recently described in melanoma (10, 25). Consistently with this hypothesis, we observed a very low rate of PD-1$^+$ NSCLC cells when in the steady monolayer culture conditions, raising up to more relevant levels when cultured in stemness conditions to form pneumospheres. Furthermore, PD-1$^+$ NSCLC cells were found significantly enriched among tumor cells surviving chemotherapy with CDDP *in vitro*, paralleled by the enhanced expression of the membrane transporter ABCG2 associated with multidrug resistance (49–52). The presence of PD-1$^+$ NSCLC cells has probably to be considered as a dynamic entity that may play relevant roles at certain times of the natural and clinical tumor history. The PD-1 receptor may actively and timely promote the preservation and regeneration of a stem-like subset within bulk NSCLC cells. In line with this speculative consideration, PD-1 engagement by its cognate ligand PD-L1 was functionally capable of enhancing the formation of stem-like pneumospheres. Conversely, the protumoral activity mediated by PD-L1 was effectively

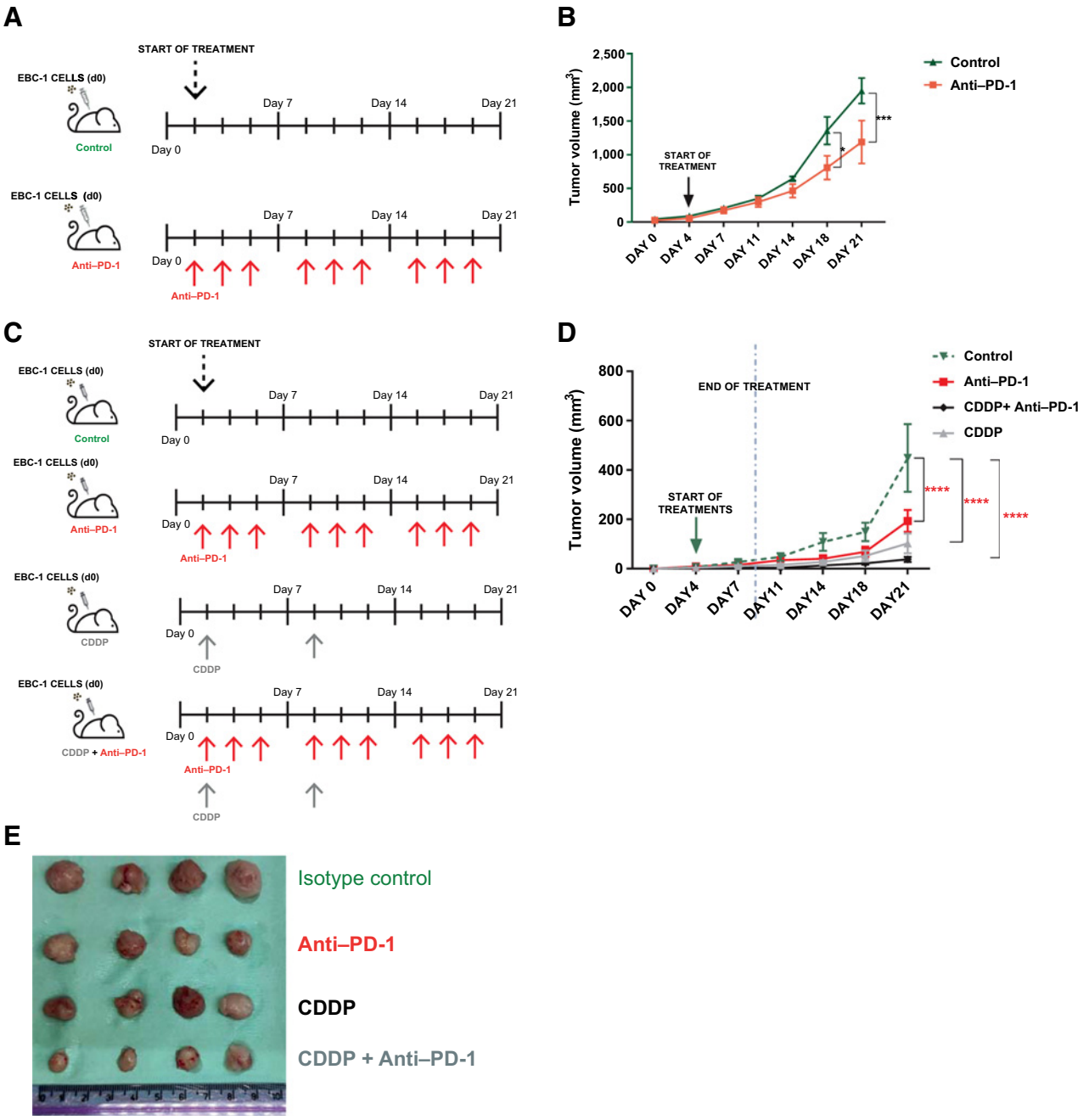

Figure 5.

Anti–PD-1 blocking antibody is capable of lymphocyte-independent antitumor activity against NSCLC xenografts. The schematic experimental design of anti–PD-1 treatment in the immunodeficient EBC-1 NSCLC xenograft model is reported (**A**). Monotherapy with anti–PD-1 antibody significantly delayed tumor growth without any contribution by the immune system ($P = 0.0006$; **B**). The schematic experimental design of anti–PD-1 treatment in the immunodeficient H1975 NSCLC xenograft model is reported (**C**). The antitumor activity by Ab anti–PD-1 was comparable with that observed with CDDP monotherapy ($P = 0.3$). The combination of Ab anti–PD-1 with CDDP significantly enhanced the antitumor activity and delayed the onset of chemoresistance compared with anti–PD-1 Ab as monotherapy ($P = 0.012$; **D**). Explanted tumor at the end of the experiment (day 21; **E**). All results were analyzed by two-way ANOVA and the Bonferroni posttest; statistical significance is reported as *, $P \leq 0.05$; **, $P \leq 0.01$; ***, $P \leq 0.001$; and ****, $P \leq 0.0001$.

impaired by the anti–PD-1 blocking antibody or, alternatively, downmodulating its expression by genetic interference. As for the downstream signaling, in our study the pathway seems similar to what described by Kleffel and colleagues in melanoma (10), with anti–PD-1 antibody inducing the reduction of tumor pS6 in PD-1$^+$ tumor cells. The protumoral role of PD-1, in stem-like conditions, is also supported by the panel of genes that we observed to be modulated in NSCLC pneumospheres by the PD-L1 stimulation,

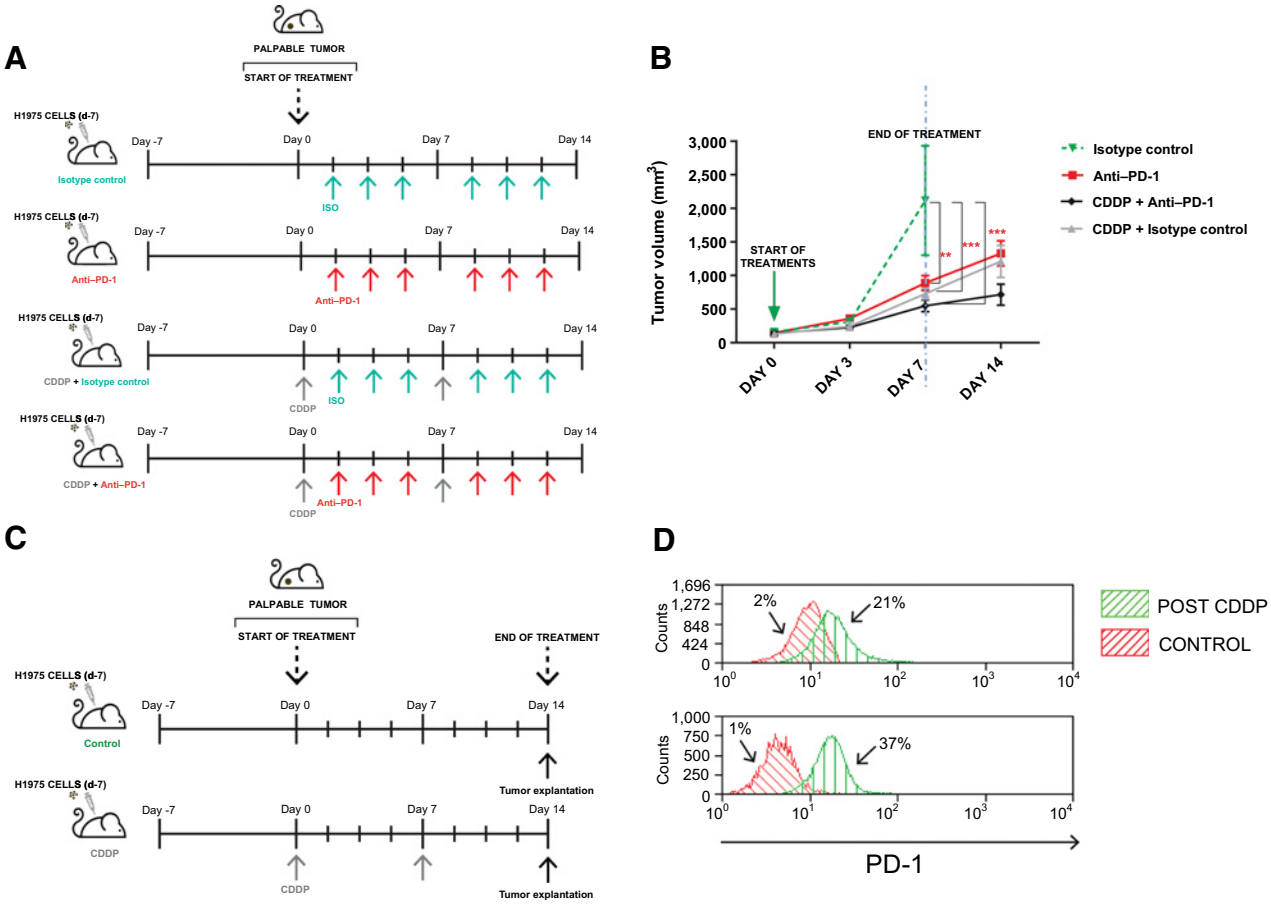

Figure 6.

Anti–PD-1 blocking antibody is capable of lymphocyte-independent antitumor activity against established and palpable NSCLC xenograft. The schematic experimental design of anti–PD-1 treatment in combination with CDDP in the immunodeficient H1975 NSCLC model is reported (**A**). Treatment with anti–PD-1 antibody delayed tumor growth of established NSCLC xenografts (H1975; $P = 0.003$) in a lymphocyte-independent manner. The antitumor activity by Ab anti–PD-1 was comparable with that observed with CDDP monotherapy ($P = 0.9$). The combination of Ab anti–PD-1 with CDDP trended toward a further enhancement of the antitumor activity and delayed the onset of chemoresistance (**B**). Schematic representation of the H1975 NSCLC xenograft model to explore the enrichment of PD-1$^+$ NSCLC after *in vivo* treatment with CDDP (**C**). PD-1$^+$ NSCLC cells significantly increased after *in vivo* treatment with CDDP as compared with untreated control ($P = 0.03$; **D**). All results were analyzed by two-way ANOVA and the Bonferroni posttest; statistical significance is reported as *, $P \leq 0.05$; **, $P \leq 0.01$; ***, $P \leq 0.001$; and ****, $P \leq 0.0001$.

mostly functionally implicated in carcinogenesis and various cancer aggressiveness processes. These data provide bases for dedicated functional and targeting investigations.

The potential clinical relevance of these observations may be envisioned in those clinical scenarios where an active role for putative cancer stem cells (CSC) may be evoked. For instance, disease relapse, following clinical response to chemotherapy, is a common and relevant problem that has been related to putative chemo-persistent CSCs. Within this hypothetical context, the central finding and message emerging from the study is the lymphocyte-independent antitumor activity played by anti–PD-1 blocking antibodies and its possible exploitation in combinations with CDDP. Our data, both *in vitro* and *in vivo* support the proof of concept that PD-1 blocking antibody exerts indeed a direct antitumor activity and may cooperate with conventional chemotherapy delaying NSCLC recovery following therapeutic CDDP. The rational basis for such cooperation was confirmed *in vivo*, by the observed relative enrichment of PD-1$^+$ NSCLC cells in tumor xenografts explanted after CDDP, indirectly supporting the chemoresistance of PD-1$^+$ NSCLC cells. The potential interference of ADCC with the observed results is negligible, as in our model the NSG mice lack functional natural killer cells and macrophages. In clinical perspective, it will be however important to confirm our preclinical findings with the anti–PD-1 antibodies approved for clinical use, as well as testing whether similar results are obtained with anti-PD-L1 Abs.

In a clinical perspective, it would be conceivable to explore the activity of anti–PD-1 therapy sequentially to chemotherapy, to contrast the residual and persistent PD-1$^+$ NSCLC cells and counteract their promotion of disease relapse. Probably, the best inhibitory effect against tumor-intrinsic PD-1 could take place during the initial tumor growth (or regrowth) phases, likely the time when putative CSC are called into action.

Interesting considerations may be related to the source of PD-1 stimulation within the tumor bulk. The activating PD-1 binding by PD-L1 may originate by the surrounding tumor cells or even by the immune infiltrating elements.

The expression of PD-L1 by tumors is known to be mainly an inducible process, and less frequently it is constitutively regulated at the genetic level (53, 54). The main inducers of PD-L1 transcription and expression are IFNs that, in most of the cases, are released by the surrounding lymphocytes as expression of an ongoing antitumor immune response. Therefore, it is conceivable that biological events, such as inflammation following chemotherapy or lymphocyte activation by checkpoint inhibitors, may enhance the production of IFNs at the tumor interface promoting PD-L1/2 expression and potentially triggering tumor-intrinsic PD-1.

This could suggest the existence of determined biological time frames when tumor-intrinsic PD-1 plays a relevant function for the tumor homeostasis and may consequently be a target for its therapeutic inhibition.

We confirmed that the tumor membrane expression of PD-L1 and PD-L2 in our NSCLC cell lines was intensely enhanced by treatment with IFNγ (Supplementary Fig. S3A), supporting the hypothesis that PD-1 stimulation may be enhanced during inflammatory processes. Our data highlight how PD-L2 is intensely expressed by NSCLC cells, suggesting the opportunity and need for specific studies to investigate its functional immunoregulatory role, possible targeting but even its potential tumor-intrinsic signaling.

Overall, the role of tumor-intrinsic PD-1 in NSCLC is complex, potentially heterogeneous and context dependent. Its comprehension is likely at the beginning. It is functionally linked and dependent on multiple dynamic variables that will require dedicated translational studies. For instance, recent reports associated the tumor-intrinsic PD-1 with tumor-suppressive functions, potentially mediating resistance to anti–PD-1 therapy or even hyperprogression (16, 17), with data apparently discordant with our findings. In particular, it was reported the tumor activation of pAKT following PD-1 blockade, resulting in the promotion of tumor growth (17). A possible speculative interpretation of such differences may be related to our stem-like experimental context. Indeed, we could observe *in vitro* the inhibitory activity of anti–PD-1 Ab only in the context of stem-like pneumospheres. Furthermore, the inhibition of pS6 that we observed in PD-1$^+$ NSCLC cells with anti–PD-1 Ab appears to be AKT independent, as we could not detect reductions but instead a modest increase of pAKT following PD-1 blockade. Dedicated studies may investigate whether, in peculiar tumorigenesis conditions where the stem-like compartment becomes activated, there may be a leading pS6 activation by an AKT-independent pathway.

Other emerging issues and opportunities for further studies include the impact of different genetic backgrounds (e.g., EGFR mutations) or the biological variables associated with specific time frames when tumor homeostasis may be altered like we saw following chemotherapy.

These functional interpretative efforts may get even more complex, though very intriguing, considering the recent descriptions of cancer cell–intrinsic PD-L1 signaling, regulating key processes like tumor growth, survival pathways, stemness, immune effects, DNA damage, drug resistance (55, 56). It will be important to explore how and whether some of these effects may be modulated by the interaction with tumor-intrinsic PD-1 and consequently by anti–PD-1 Abs. For instance, evidence in triple-negative breast cancer, support that tumor-intrinsic PD-L1 regulates tumor progression and EMT by p38-MAPK pathway and this process may be activated by PD-1 (57).

Preliminary data from our group (Supplementary Fig. S3B) also suggest a reduction of phospho-p38 MAPK in NSCLC cells by anti–PD-1 Abs, suggesting that such an effect may also tap into the interactions with tumor-intrinsic PD-1, opening to speculations and investigations to demonstrate the existence of a similar pathway also in lung cancer.

While confirming the important role of tumor-intrinsic PD-1, all these considerations and sometimes heterogenous reports, call for caution in its biological interpretation and possible therapeutic exploitation.

Overall, we reported a novel, lymphocyte-independent, antitumor activity of PD-1 blocking antibody against NSCLC.

While the "conventional" lymphocyte centric activity of anti–PD-1 blockade remains the mainstay immunotherapy mechanism to attack bulk tumors, our study provides translational rationale to imagine and explore an additional and/or integrative tumor-directed effect, possibly relevant to counteract challenging clinical settings sustained by tumor cell subsets with stemness features.

Authors' Disclosures

M.C. De Santis reports other support from Fondazione Umberto Veronesi during the conduct of the study. L. D'Ambrosio reports advisory board participation with GSK, AstraZeneca, Eisai, and PSI CRO, Italy, and meeting participation with PharmaMar. G. Grignani reports grants and personal fees from Bayer, Novartis, and Pharmamar and personal fees from Merck, Esai, and Lilly outside the submitted work. E. Hirsch reports grants from Piattaforma regionale DEFLECT-320-44 during the conduct of the study as well as other support from Kither Biotech Srl outside the submitted work; in addition, E. Hirsch is founder, shareholder, and advisor of Kither Biotech Srl, a pharmaceutical product company developing PI3K inhibitors for the treatment of respiratory diseases. G.V. Scagliotti reports personal fees from Eli Lilly, AstraZeneca, Pfizer, MSD, Johnson & Johnson, Takeda, BeiGene, and Verastem outside the submitted work. S. Novello reports personal fees from AstraZeneca, AMG, BI, Lilly, Roche, Pfizer, Takeda, Novartis, MSD, and Thermo Fisher Scientific outside the submitted work. P. Bironzo reports personal fees from AstraZeneca, Bristol Myers Squibb, Roche, BeiGene, and Takeda; grants from Roche and Pfizer; and other support from Amgen and Daiichi Sankyo outside the submitted work. D. Sangiolo reports grants from "Associazione Italiana Ricerca sul Cancro" (AIRC), FPRC ONLUS, and Ministero della Salute during the conduct of the study as well as other support from Roche and GSK outside the submitted work. No disclosures were reported by the other authors.

Authors' Contributions

R. Rotolo: Validation, investigation, writing–original draft, writing–review and editing. **V. Leuci:** Conceptualization, investigation, writing–original draft, writing–review and editing. **C. Donini:** Investigation, visualization, writing–original draft, writing–review and editing. **F. Galvagno:** Conceptualization, investigation, writing–review and editing. **A. Massa:** Data curation, formal analysis, investigation, methodology, writing–review and editing. **M.C. De Santis:** Data curation, formal analysis, investigation, methodology, writing–review and editing. **S. Peirone:** Data curation, formal analysis, investigation, methodology, writing–review and editing. **G. Medico:** Investigation, writing–review and editing. **M. Sanlorenzo:** Conceptualization, investigation, writing–review and editing. **I. Vujic:** Resources, writing–review and editing. **L. Gammaitoni:** Resources, funding acquisition, writing–review and editing. **M. Basiricò:** Resources, investigation, writing–review and editing. **L. Righi:** Resources, writing–review and editing. **C. Riganti:** Resources, funding acquisition, writing–review and editing. **I.C. Salaroglio:** Resources, investigation, writing–review and editing. **F. Napoli:** Investigation, writing–review and editing. **F. Tabbò:** Resources, writing–review and editing. **A. Mariniello:** Resources, writing–review and editing. **E. Vigna:** Resources, investigation, writing–review and editing. **C. Modica:** Resources, funding acquisition, investigation, writing–review and editing. **L. D'Ambrosio:** Resources, writing–review and editing. **G. Grignani:** Conceptualization, resources, supervision, funding acquisition, writing–original draft, project administration, writing–review and editing. **R. Taulli:** Funding acquisition, writing–review and editing. **E. Hirsch:** Data curation, writing–review and editing. **M. Cereda:** Data curation, formal analysis, investigation, methodology, writing–review and editing. **M. Aglietta:** Resources, data curation, formal analysis, investigation, methodology, writing–review and editing. **G.V. Scagliotti:** Resources, data curation, formal analysis, funding acquisition, investigation,

methodology, writing–review and editing. **S. Novello:** Resources, investigation, writing–review and editing. **P. Bironzo:** Resources, investigation, writing–review and editing. **D. Sangiolo:** Conceptualization, resources, data curation, supervision, funding acquisition, writing–original draft, project administration, writing–review and editing.

Acknowledgments

This study was supported by fundings from "Associazione Italiana Ricerca sul Cancro" (AIRC) IG-2017 n. 20259 (D. Sangiolo); AIRC IG-2019 n. 23760 (G.V. Scagliotti); AIRC IG-2018 n. 21408 (C. Riganti); AIRC IG-2021 n.25978 (R. Taulli); FPRC ONLUS 5 × 1000, Ministero della Salute 2015 Cancer ImGen (D. Sangiolo); MESOLINE Project funded by ASO Alessandria (G.V. Scagliotti); Ricerca Corrente Ministero Salute 2022 (D. Sangiolo, G. Grignani).

The publication costs of this article were defrayed in part by the payment of publication fees. Therefore, and solely to indicate this fact, this article is hereby marked "advertisement" in accordance with 18 USC section 1734.

Note

Supplementary data for this article are available at Clinical Cancer Research Online (http://clincancerres.aacrjournals.org/).

Received March 13, 2022; revised August 18, 2022; accepted September 16, 2022; published first September 27, 2022.

References

1. Sharma P, Allison JP. The future of immune checkpoint therapy. Science 2015;348:56–61.
2. Alsaab HO, Sau S, Alzhrani R, Tatiparti K, Bhise K, Kashaw SK, et al. PD-1 and PD-L1 checkpoint signaling inhibition for cancer immunotherapy: mechanism, combinations, and clinical outcome. Front Pharmacol 2017;8:561.
3. Blank C, Gajewski TF, Mackensen A. Interaction of PD-L1 on tumor cells with PD-1 on tumor-specific T cells as a mechanism of immune evasion: implications for tumor immunotherapy. Cancer Immunol Immunother 2005;54:307–14.
4. Chemnitz JM, Parry RV, Nichols KE, June CH, Riley JL. SHP-1 and SHP-2 associate with immunoreceptor tyrosine-based switch motif of programmed death 1 upon primary human T cell stimulation, but only receptor ligation prevents T cell activation. J Immunol 2004;173:945–54.
5. Chen L, Han X. Anti-PD-1/PD-L1 therapy of human cancer: past, present, and future. J Clin Invest 2015;125:3384–91.
6. Freeman GJ, Long AJ, Iwai Y, Bourque K, Chernova T, Nishimura H, et al. Engagement of the PD-1 immunoinhibitory receptor by a novel B7 family member leads to negative regulation of lymphocyte activation. J Exp Med 2000;192:1027–34.
7. Riley JL. PD-1 signaling in primary T cells. Immunol Rev 2009;229:114–25.
8. Tumeh PC, Harview CL, Yearley JH, Shintaku IP, Taylor EJ, Robert L, et al. PD-1 blockade induces responses by inhibiting adaptive immune resistance. Nature 2014;515:568–71.
9. Yao H, Wang H, Li C, Fang JY, Xu J. Cancer cell-intrinsic PD-1 and implications in combinatorial immunotherapy. Front Immunol. 2018;9:1774.
10. Kleffel S, Posch C, Barthel SR, Mueller H, Schlapbach C, Guenova E, et al. Melanoma cell-intrinsic PD-1 receptor functions promote tumor growth. Cell 2015;162:1242–56.
11. Schatton T, Schütte U, Frank NY, Zhan Q, Hoerning A, Robles SC, et al. Modulation of T-cell activation by malignant melanoma initiating cells. Cancer Res 2010;70:697–708.
12. Zhao Y, Harrison DL, Song Y, Ji J, Huang J, Hui E. Antigen-presenting cell-intrinsic PD-1 neutralizes PD-L1 in cis to attenuate PD-1 signaling in T cells. Cell Rep 2018;24:379–90.
13. Torabi A, Amaya CN, Wians FH, Bryan BA. PD-1 and PD-L1 expression in bone and soft tissue sarcomas. Pathology 2017;49:506–13.
14. Li H, Li X, Liu S, Guo L, Zhang B, Zhang J, et al. Programmed cell death-1 (PD-1) checkpoint blockade in combination with a mammalian target of rapamycin inhibitor restrains hepatocellular carcinoma growth induced by hepatoma cell-intrinsic PD-1. Hepatology 2017;66:1920–33.
15. Pu N, Gao S, Yin H, Li JA, Wu W, Fang Y, et al. Cell-intrinsic PD-1 promotes proliferation in pancreatic cancer by targeting CYR61/CTGF via the hippo pathway. Cancer Lett 2019;460:42–53.
16. Du S, McCall N, Park K, Guan Q, Fontina P, Ertel A, et al. Blockade of tumor-expressed PD-1 promotes lung cancer growth. Oncoimmunology 2018;7:e1408747.
17. Wang X, Yang X, Zhang C, Wang Y, Cheng T, Duan L, et al. Tumor cell-intrinsic PD-1 receptor is a tumor suppressor and mediates resistance to PD-1 blockade therapy. Proc Natl Acad Sci U S A 2020;117:6640–50.
18. Duma N, Santana-Davila R, Molina JR. Non-small cell lung cancer: epidemiology, screening, diagnosis, and treatment. Mayo Clin Proc 2019;94:1623–40.
19. Reck M, Mok TSK, Nishio M, Jotte RM, Cappuzzo F, Orlandi F, et al. Atezolizumab plus bevacizumab and chemotherapy in non-small-cell lung cancer (IMpower150): key subgroup analyses of patients with EGFR mutations or baseline liver metastases in a randomised, open-label phase 3 trial. Lancet Respir Med 2019;7:387–401.
20. Mok TSK, Wu YL, Kudaba I, Kowalski DM, Cho BC, Turna HZ, et al. Pembrolizumab versus chemotherapy for previously untreated, PD-L1-expressing, locally advanced or metastatic non-small-cell lung cancer (KEYNOTE-042): a randomised, open-label, controlled, phase 3 trial. Lancet 2019;393:1819–30.
21. Gandhi L, Rodríguez-Abreu D, Gadgeel S, Esteban E, Felip E, De Angelis F, et al. Pembrolizumab plus chemotherapy in metastatic non-small-cell lung cancer. N Engl J Med 2018;378:2078–92.
22. Brody R, Zhang Y, Ballas M, Siddiqui MK, Gupta P, Barker C, et al. PD-L1 expression in advanced NSCLC: insights into risk stratification and treatment selection from a systematic literature review. Lung Cancer 2017;112:200–15.
23. Malhotra J, Jabbour SK, Aisner J. Current state of immunotherapy for non-small cell lung cancer. Transl Lung Cancer Res 2017;6:196–211.
24. Reck M, Rodríguez-Abreu D, Robinson AG, Hui R, Csőszi T, Fülöp A, et al. Pembrolizumab versus chemotherapy for PD-L1-positive non-small-cell lung cancer. N Engl J Med 2016;375:1823–33.
25. Sanlorenzo M, Vujic I, Floris A, Novelli M, Gammaitoni L, Giraudo L, et al. BRAF and MEK inhibitors increase PD-1-positive melanoma cells leading to a potential lymphocyte-independent synergism with anti-PD-1 antibody. Clin Cancer Res 2018;24:3377–85.
26. Frankish A, Diekhans M, Ferreira AM, Johnson R, Jungreis I, Loveland J, et al. GENCODE reference annotation for the human and mouse genomes. Nucleic Acids Res 2019;47:D766–D73.
27. Dobin A, Davis CA, Schlesinger F, Drenkow J, Zaleski C, Jha S, et al. STAR: ultrafast universal RNA-seq aligner. Bioinformatics 2013;29:15–21.
28. Liao Y, Smyth GK, Shi W. FeatureCounts: an efficient general purpose program for assigning sequence reads to genomic features. Bioinformatics 2014;30:923–30.
29. Zhang Y, Parmigiani G, Johnson WE. Batch effect adjustment for RNA-seq count data. NAR Genom Bioinform 2020;2:lqaa078.
30. Love MI, Huber W, Anders S. Moderated estimation of fold change and dispersion for RNA-seq data with DESeq2. Genome Biol 2014;15:550.
31. Qiu X, Wang Z, Li Y, Miao Y, Ren Y, Luan Y. Characterization of sphere-forming cells with stem-like properties from the small cell lung cancer cell line H446. Cancer Lett 2012;323:161–70.
32. Herreros-Pomares A, de-Maya-Girones JD, Calabuig-Fariñas S, Lucas R, Martínez A, Pardo-Sánchez JM, et al. Lung tumorspheres reveal cancer stem cell-like properties and a score with prognostic impact in resected non-small-cell lung cancer. Cell Death Dis 2019;10:660.
33. Moncho-Amor V, Ibañez de Cáceres I, Bandres E, Martínez-Poveda B, Orgaz JL, Sánchez-Pérez I, et al. DUSP1/MKP1 promotes angiogenesis, invasion and metastasis in non-small-cell lung cancer. Oncogene 2011;30:668–78.
34. Souglakos J, Boukovinas I, Taron M, Mendez P, Mavroudis D, Tripaki M, et al. Ribonucleotide reductase subunits M1 and M2 mRNA expression levels and clinical outcome of lung adenocarcinoma patients treated with docetaxel/gemcitabine. Br J Cancer 2008;98:1710–5.

35. Boukovinas I, Papadaki C, Mendez P, Taron M, Mavroudis D, Koutsopoulos A, et al. Tumor BRCA1, RRM1 and RRM2 mRNA expression levels and clinical response to first-line gemcitabine plus docetaxel in non-small-cell lung cancer patients. PLoS One 2008;3:e3695.
36. Zhao J, Li H, Yuan M. EGR1 promotes stemness and predicts a poor outcome of uterine cervical cancer by inducing SOX9 expression. Genes Genomics 2021;43: 459–70.
37. Chiang K, Zielinska AE, Shaaban AM, Sanchez-Bailon MP, Jarrold J, Clarke TL, et al. PRMT5 is a critical regulator of breast cancer stem cell function via histone methylation and FOXP1 expression. Cell Rep 2017; 21:3498–513.
38. Muhammad N, Bhattacharya S, Steele R, Phillips N, Ray RB. Involvement of c-Fos in the promotion of cancer stem-like cell properties in head and neck squamous cell carcinoma. Clin Cancer Res 2017;23: 3120–8.
39. Apostolou P, Toloudi M, Ioannou E, Chatziioannou M, Kourtidou E, Vlachou I, et al. AP-1 gene expression levels may be correlated with changes in gene expression of some stemness factors in colon carcinomas. J Signal Transduct 2013;2013:497383.
40. Chang CC, Hsu WH, Wang CC, Chou CH, Kuo MY, Lin BR, et al. Connective tissue growth factor activates pluripotency genes and mesenchymal-epithelial transition in head and neck cancer cells. Cancer Res 2013;73:4147–57.
41. Chien W, Yin D, Gui D, Mori A, Frank JM, Said J, et al. Suppression of cell proliferation and signaling transduction by connective tissue growth factor in non-small cell lung cancer cells. Mol Cancer Res 2006;4:591–8.
42. Han Y, Song C, Wang J, Tang H, Peng Z, Lu S. HOXA13 contributes to gastric carcinogenesis through DHRS2 interacting with MDM2 and confers 5-FU resistance by a p53-dependent pathway. Mol Carcinog 2018;57:722–34.
43. Wu S, Guo X, Zhou J, Zhu X, Chen H, Zhang K, et al. High expression of UNC5B enhances tumor proliferation, increases metastasis, and worsens prognosis in breast cancer. Aging 2020;12:17079–98.
44. Boles NC, Hirsch SE, Le S, Corneo B, Najm F, Minotti AP, et al. NPTX1 regulates neural lineage specification from human pluripotent stem cells. Cell Rep 2014;6: 724–36.
45. Yan H, Zheng C, Li Z, Bao B, Yang B, Hou K, et al. NPTX1 promotes metastasis via integrin/FAK signaling in gastric cancer. Cancer Manag Res 2019;11:3237–51.
46. Givant-Horwitz V, Davidson B, Goderstad JM, Nesland JM, Tropé CG, Reich R. The PAC-1 dual specificity phosphatase predicts poor outcome in serous ovarian carcinoma. Gynecol Oncol 2004;93:517–23.
47. Hou PC, Li YH, Lin SC, Lee JC, Lin BW, Liou JP, et al. Hypoxia-induced downregulation of DUSP-2 phosphatase drives colon cancer stemness. Cancer Res 2017;77:4305–16.
48. Healy S, Khan P, Davie JR. Immediate early response genes and cell transformation. Pharmacol Ther 2013;137:64–77.
49. Merk J, Rolff J, Dorn C, Leschber G, Fichtner I. Chemoresistance in non-small-cell lung cancer: can multidrug resistance markers predict the response of xenograft lung cancer models to chemotherapy? Eur J Cardiothorac Surg 2011;40:e29–33.
50. Krishnamurthy P, Schuetz JD. Role of ABCG2/BCRP in biology and medicine. Annu Rev Pharmacol Toxicol 2006;46:381–410.
51. Barr MP, Gray SG, Hoffmann AC, Hilger RA, Thomale J, O'Flaherty JD, et al. Generation and characterisation of cisplatin-resistant non-small cell lung cancer cell lines displaying a stem-like signature. PLoS One 2013;8:e54193.
52. Dean M, Fojo T, Bates S. Tumour stem cells and drug resistance. Nat Rev Cancer 2005;5:275–84.
53. Garcia-Diaz A, Shin DS, Moreno BH, Saco J, Escuin-Ordinas H, Rodriguez GA, et al. Interferon receptor signaling pathways regulating PD-L1 and PD-L2 expression. Cell Rep 2017;19:1189–201.
54. Martin V, Chiriaco C, Modica C, Acquadro A, Cortese M, Galimi F, et al. Met inhibition revokes IFNγ-induction of PD-1 ligands in MET-amplified tumours. Br J Cancer 2019;120:527–36.
55. Kornepati AVR, Vadlamudi RK, Curiel TJ. Programmed death ligand 1 signals in cancer cells. Nat Rev Cancer 2022;22:174–89.
56. Kornepati AVR, Boyd JT, Murray CE, Saifetiarova J, de la Peña Avalos B, Rogers CM, et al. Tumor Intrinsic PD-L1 promotes DNA repair in distinct cancers and suppresses PARP inhibitor-induced synthetic lethality. Cancer Res 2022;82: 2156–70.
57. Chen C, Li S, Xue J, Qi M, Liu X, Huang Y, et al. PD-L1 tumor-intrinsic signaling and its therapeutic implication in triple-negative breast cancer. JCI Insight 2021; 6:e131458.